Program Digest, 2019 IEEE International Ultrasonics Symposium (IUS)
Glasgow, Scotland, October 6-9, 2019

Hybrid Filter Design for 5G using IPD and Acoustic Technologies

Chengjie Zuo[1,2], Chenggong He[2], Wei Cheng[2], Zheng Wang[2]
[1]*School of Microelectronics, University of Science and Technology of China, Hefei, China*
[2]*YUNTA Technologies and ANUKI Technologies, Hefei, China*
czuo@ustc.edu.cn

***Abstract*—For the first time, a hybrid filter design approach based on the combination of Integrated Passive Device (IPD) and acoustic technologies is proposed to satisfy the new demands in 5G New Radio (NR) applications, where high frequency (above 3 GHz) and wide bandwidth (up to 900 MHz to date) are defined by the standards. The Band n77 filter is used as an extreme example to demonstrate the capability to achieve high operating frequency from 3.3 to 4.2 GHz, wide bandwidth of 900 MHz, high rejection of 36 dB at 200 MHz away, and low insertion loss of 2.5 dB.**

Keywords—hybrid filter, IPD, acoustic filter, 5G NR

I. Introduction

There has been a general and inevitable trend of utilizing higher frequency and wider bandwidth of the electromagnetic spectrum for 5G New Radio (NR) wireless communications. For example, 27.5 to 28.35 GHz with bandwidth of 850 MHz has been identified as one of the 5G bands in the US, while one of the 5G bands is 3.3 to 3.6 GHz with bandwidth of 300 MHz in China. Not only the higher carrier frequency but also the much wider bandwidth pose significant challenges on the RF front end: antennas, power amplifiers and especially filters. Although acoustic technologies, like the Film Bulk Acoustic Wave Resonator (FBAR) [1] and Solidly Mounted Resonator (SMR) [2] filters, both called Bulk Acoustic Wave (BAW), and the Surface Acoustic Wave (SAW) [3-5] filters, have advanced rapidly nowadays, it is still very difficult to keep up with the updates in wireless standards. Therefore, the wireless industry calls for next-generation technology solutions to meet the new system requirements in 5G: carrier aggregation, MIMO, high frequency and wide bandwidth filtering.

This paper presents a new design methodology of having both lumped-LC Integrated Passive Device (IPD) and high-Q acoustic resonant technologies to achieve wide bandwidth and sharp roll-off at the same time. IPD inductors and capacitors are used to form a wide passband, while acoustic resonators provide sharp roll-off and high rejection at band edges. As a proof of concept, this paper selects Band n77 as an extreme case to show how a wide bandwidth of 900 MHz at 3.75GHz can be realized by combining IPD and acoustic technologies.

II. Integrated Passive Device

Integrated Passive Device (IPD) technology dates back to 1967 [6], where tantalum, tantalum pentoxide, and nichrome-gold were used to fabricate resistors, capacitors, and inductors, respectively, on an integrated circuit. The quality factor (Q) was reported to be about 15 at 50 MHz for a 50 pF capacitor, while the inductor Q was measured between 15 and 20 at 10 MHz for 1 μH occupying 0.35 inches square. With Moore's law, active devices, i.e., transistors, have been scaled down to nanometer level over the years, while, on the other hand, it is very difficult to shrink passive device (especially inductors) dimensions and maintain high performance at the same time. Early attempts to integrate passive devices on Silicon (Si) substrates struggled a lot with parasitic effects simply due to the fact that Silicon is semiconductor. Even by adding a thick oxide layer to isolate inductors from the Si substrate, the achieved Q was below 10 for 1.9 nH and 9.7 nH at GHz frequencies [7]. Until late 1990s, researchers were able to achieve inductor Q (Q_{max}) larger than 20 by adopting exotic substrates, like high-resistivity Silicon (HRS), sapphire, and quartz [8, 9], or even fabricating Micro-Electro-Mechanical Systems (MEMS) structures to suspend inductor coils above substrate [8, 10].

Compared with MEMS and other alternative solutions, the HRS IPD technology is more compatible with CMOS foundry and also has much better manufacturability, so it attracts a lot of attention from the industry. Several companies developed and commercialized their variant of the HRS IPD technology independently [11-14], showing inductor Q around 25 in the 1 to 2 GHz range. However, the wideband filter market has been dominated by the Low-Temperature Co-fired Ceramic (LTCC) technology [15, 16], where Q can be up to 50 for inductors. In order for HRS IPD to deliver the same level of performance as (or higher than) LTCC, we performed a series of simulations to study the most critical factor in determining IPD inductor Q, as shown in Figs. 1-3. We find out that as long as the substrate resistivity is above 1 kΩ·cm, it is the coil metal thickness that becomes dominant for inductor Q, while further increasing the substrate resistivity doesn't help much. Fig. 3 also proves that HRS IPD can deliver high Q over 60 even at 1 GHz, if 50 μm thick metal is available for inductor design.

In terms of capacitor for RF application, IPD has a natural advantage over LTCC, simply because it is based on thin-film processing instead of multi-layer ceramic sheet lamination [16] and the capacitance density in IPD is much higher than LTCC. Especially for higher frequencies above 3 GHz as required by 5G, higher capacitance density means smaller capacitor area and therefore less parasitic resistance and inductance coming from interconnects, which makes IPD thin-film based metal-insulator-metal (MIM) capacitors intrinsically have higher Q and resonant frequency. Considering all these, IPD stands out as a very promising technology for wide-bandwidth, low-loss, and small-size filtering solutions at frequencies above 3 GHz for 5G and future wireless communications.

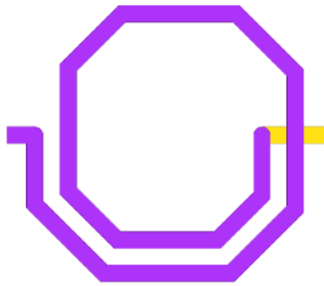

Fig. 1. Top-view of the 3 nH IPD inductor on HRS substrate under study.

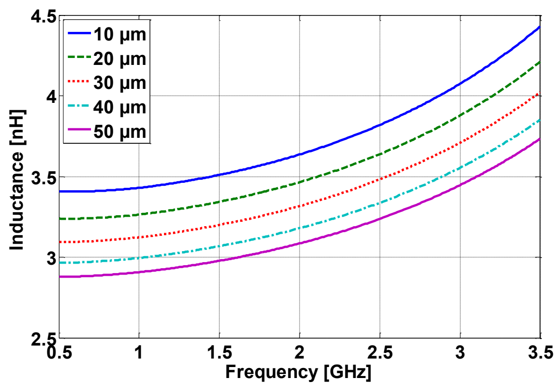

Fig. 2. Simulated inductance plotted as a function of frequency and coil metal thickness varied from 10 μm to 50 μm (Cu).

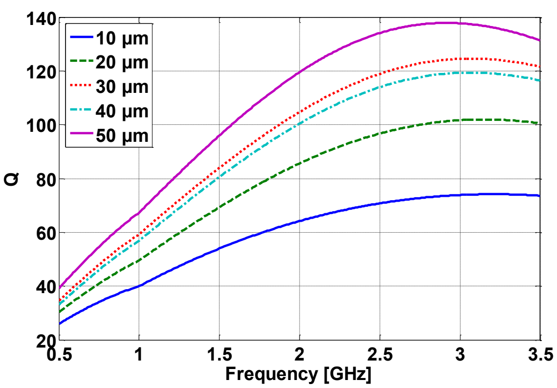

Fig. 3. Simulated inductor Q plotted as a function of frequency and coil metal thickness varied from 10 μm to 50 μm (Cu).

III. Acoustic Technologies for Wideband

Acoustic technologies are well known to deliver very high Q (> 1000) within a very small volume, which makes acoustic filters indispensable in today's smartphones where more than 80 SAW/BAW filters are used to support more than 40 bands worldwide. Recent demonstrations show Q values even above 7000 for novel SAW structures [5, 17, 18]. While Q value was enhanced significantly over the years, researchers have been looking for ways to increase the electromechanical coupling coefficient (k^2) as well, because it determines the maximum relative bandwidth that can be achieved for ladder-type filters based on acoustic resonators [19].

Several approaches have been pursued in parallel, and one of the successful attempts was to dope or alloy piezoelectric Aluminum Nitride (AlN) with exotic materials, such as Sc [20, 21], MgZr [22], or CrN [23]. Although many studies have shown enhanced piezoelectric coefficient (d_{33}) from material point of view and 4 times improvement in electromechanical coupling coefficient (k^2) in laterally vibrating resonators from device point of view [24-26], there is no demonstration to date that delivers high coupling coefficient ($k^2 > 10\%$) with decent Q (> 1000) and operating frequency above 3 GHz as required by 5G standards.

Besides changing the material, another way is to look at different resonant or mechanical modes that can be possibly excited in AlN, as proposed in [27]. Traditionally in BAW [1, 2] and Contour-Mode Resonator (CMR) [24], researchers had been focusing on one-dimensional (1D) mode in thickness or lateral direction, or designing mode shape in top view of the resonator structure, while in the case of Cross-sectional Mode Resonator (XMR) [27] a two-dimensional (2D) mode shape is excited in the cross-sectional view of the resonator, so that the longitudinal and transverse piezoelectric coefficients (d_{33} and d_{31}) are coherently combined and harnessed to transduce one single mechanical vibration mode. In this way, the k^2 of XMR has contributions from both d_{33} and d_{31} and can add up to 10% for AlN resonators. The XMR concept has been under a lot of development [28-30] and the operating frequency can be up to 3.5 GHz [31] reaching the 5G frequency range with $Q > 1000$. However, the demonstrated k^2 has been limited below 7% in hardware mainly due to challenges in today's microfabrication technology that makes the desired structures hard to realize.

A third approach is to borrow materials from SAW, but in a thin-film form produced by polishing [32], deposition [33], or ion slicing [34]. Piezoelectric MEMS resonators based on thin-film Lithium Niobate ($LiNbO_3$) were reported with operating frequency up to 4.5 GHz early in 2009 [35], and it was even shown lately to have operating frequency above 5 GHz with a surprisingly high k^2 over 26% [36]. Despite the high frequency and k^2, the resonators still need less spurious and higher Q for better use in filter designs and the C_0 or area also needs to be scaled up for impedance matching.

As can be seen, all the three technologies show promise for high frequency and high bandwidth filtering applications as required in 5G. Considering AlN doping can also be applied to XMR designs, it provides an extra degree of freedom for Q and bandwidth control by changing AlN doping concentration or resonator geometry. Therefore, it would be reasonable for us to assume k^2 of 10% and Q of 1000 in the Band n77 frequency range for the following analysis and co-designs with IPD.

IV. IPD and Acoustic Co-Design

Hybrid filter design using both lumped LC and acoustic components has been reported very recently in a few cases, where inductors and capacitors were implemented using either LTCC [37] or Surface Mount Device (SMD) [38] technology. The operating frequencies were below 3 GHz mainly for 4G LTE bands, where LTCC or SMD might be sufficient, but not good enough to deliver high performance at 5G bands above 3 GHz due to the reasons explained in Section II. Therefore, in this paper, the first hybrid filter design based on IPD passives and acoustic components is reported to realize wide bandwidth, high frequency, sharp roll-off, and low insertion loss all at the same time. The circuit schematic is shown in Fig. 4.

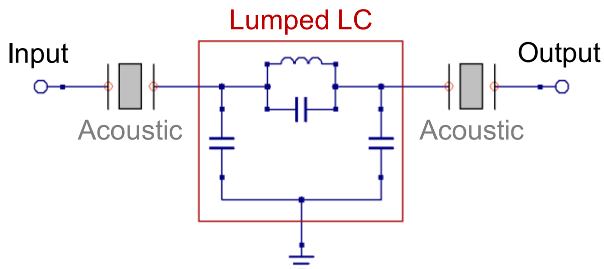

Fig. 4. Schematic of the hybrid band-pass filter (BPF) design.

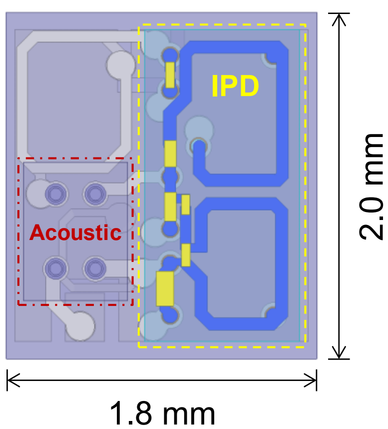

Fig. 5. Layout drawing of the Band n77 hybrid filter using IPD, acoustic, and substrate technologies.

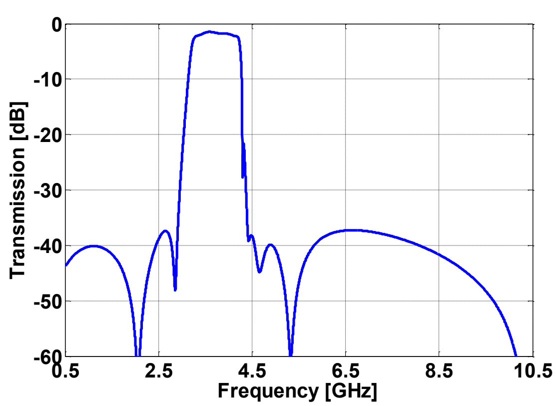

Fig. 6. Simulated transmission response of the Band n77 BPF showing wide passband of 900 MHz, low insertion loss and high rejection.

The Band n77 band-pass filter (BPF) is designed using one IPD die and one acoustic die assembled on a 4-layer laminate substrate. Two high-Q inductors and six high-Q capacitors are integrated on the IPD die with size of 1.8 x 0.9 mm, while two acoustic resonators are integrated on a second die with size of 0.8 x 0.6 mm. There are two additional inductors implemented in the metal layers available from the laminate substrate due to size constraints. The final package size is only 2.0 x 1.8 mm, as illustrated in Fig. 5, enabling a very small PCB footprint for 5G applications in mobile handsets.

The two acoustic resonators are assumed to have k^2 of 10% and Q of 1000, and the well-known BVD model [39] is used to construct the equivalent circuits of the resonators for IPD and acoustic co-design. The IPD technology has Cu layers up to 50 µm thick for high Q inductor design. The inductors and capacitors including parasitic effects are carefully simulated in HFSS® to optimize the filter transmission characteristics. As shown in Fig. 6, the out-of-band rejection is around 40 dB for the entire frequency range from 0.5 to 10.5 GHz. The insertion loss is low as 2.3 dB at 3.3 GHz and 2.5 dB at 4.2 GHz for the two edges of the 900 MHz passband. The close-in rejection is optimized for Band n79, which is the closest 5G band next to Band n77 and starts from 4.4 GHz, only 200 MHz away from the upper edge of the n77 passband. Thanks to high Q of the acoustic resonators, this hybrid filter is able to deliver 36 dB rejection at 4.4 GHz, which proves the hybrid approach is able to achieve wide passband and sharp roll-off at the same time.

Further study is conducted to evaluate the impact of Q and k^2 of the acoustic resonators on the performance of this hybrid BPF. Due to the specific circuit configuration adopted in this paper, as shown in Fig. 4, acoustic resonators are only used to create sharp roll-off at the upper edge of the passband around 4.3 GHz, while the 900 MHz passband shape and majority of the rejection notches are all maintained by the IPD part of the circuit. Therefore, higher Q or k^2 wouldn't bring much more benefit to the final filter performance, which makes the hybrid filter design less sensitive to process variations and easier for high volume manufacturing.

V. Conclusion

For the first time, a Band n77 band-pass filter design with small footprint of 2.0 x 1.8 mm is presented based on a hybrid combination of IPD, acoustic and substrate technologies in the same package. IPD inductors and capacitors are used to shape the wide passband of 900 MHz, while the high Q of acoustic resonators is required to achieve high rejection at frequencies close to the passband, like 200 MHz away. The hybrid design approach based on IPD and acoustic technologies proves to be a promising solution for 5G NR bands like n77, n78 and n79, where operating frequency is above 3 GHz and bandwidth is above 500 MHz, over 10 times wider than 4G LTE bands.

Acknowledgment

This work was partially carried out at the USTC Center for Micro and Nanoscale Research and Fabrication. The authors would like to thank the staff for precious discussions and help.

References

[1] R. Ruby and P. Merchant, "Micromachined Thin Film Bulk Acoustic Resonators," presented at the IEEE 48th Annual Symposium on Frequency Control, Boston, MA, USA, 1994.

[2] R. Aigner, J. Ella, H.-J. Timme, L. Elbrecht, W. Nessler, and S. Marksteiner, "Advancement of MEMS into RF-filter applications," presented at the 2002 IEEE International Electron Devices Meeting (IEDM 2002), San Francisco, CA, USA, 2002.

[3] R. M. Hays and C. S. Hartmann, "Surface-Acoustic-Wave Devices for Communications," *Proceedings of the IEEE,* vol. 64, pp. 652-671, 1976.
[4] M. Yamaguchi, K.-Y. Hashimoto, and H. Kogo, "Suboptimization of Electrode-Withdrawal Weighted SAW Filters," *IEEE Transactions on Sonics and Ultrasonics,* vol. 26, pp. 53-59, 1979.
[5] T. Takai, H. Iwamoto, Y. Takamine, T. Wada, M. Hiramoto, M. Koshino, and N. Nakajima, "Investigations on Design Technologies for SAW Quadplexer with Narrow Duplex Gap," presented at the 2016 IEEE MTT-S International Microwave Symposium (IMS 2016).
[6] R. Naylor and R. Fairbank, "The Preparation and Application of Tantalum Thin Film Passive Components," *Radio and Electronic Engineer,* vol. 33, pp. 229-240, April 1967.
[7] N. M. Nguyen and R. G. Meyer, "Si IC-Compatible Inductors and LC Passive Filters," *IEEE Journal of Solid-State Circuits,* vol. 25, 1990.
[8] J. N. Burghartz, "Integrated Multilayer RF Passives in Silicon Technology," presented at the 1998 Topical Meeting on Silicon Monolithic Integrated Circuits in RF Systems, Ann Arbor, MI, 1998.
[9] J. Hartung, "Integrated Passive Components in MCM-Si Technology and Their Applications in RF-Systems," presented at the 1998 International Conference on Multichip Modules and High Density Packaging, Denver, CO, USA, 1998.
[10] J.-B. Yoon, Y.-S. Choi, B.-I. Kim, Y. Eo, and E. Yoon, "CMOS-Compatible Surface-Micromachined Suspended-Spiral Inductors for Multi-GHz Silicon RF ICs," *IEEE Electron Device Letters,* 2002.
[11] K. Liu and R. C. Frye, "Full-Circuit Design Optimization of a RF Silicon Integrated Passive Device," presented at the 2006 IEEE Electrical Performane of Electronic Packaging, Scottsdale, AZ, 2006.
[12] K. Liu and R. C. Frye, "Small Form-Factor Integrated Passive Devices for SiP Applications," presented at the 2007 IEEE/MTT-S International Microwave Symposium (IMS 2007), Honolulu, HI, USA, 2007.
[13] A. C. Kundu, M. Megahed, and D. Schmidt, "Comparison and Analysis of Integrated Passive Device Technologies for Wireless Radio Frequency Module," presented at the 58th Electronic Components and Technology Conference (ECTC 2008), Lake Buena Vista, FL, 2008.
[14] F. Gianesello, C. Durand, R. Pilard, D. Petit, J. Penard, S. Jan, D. Gloria, B. Rauber, and C. Raynaud, "Integration of Cellular Front End Modules on Advanced High Resistivity SOI RF CMOS Technology," presented at the 2011 IEEE Topical Conference on Power Amplifiers for Wireless and Radio Applications, Phoenix, AZ, USA, 2011.
[15] W. Eurskens, W. Wersing, S. Gohlke, V. Wannemnacher, P. Hild, and R. Weigel, "Design and Performance of UHF Band Inductors, Capacitors and Resonators using LTCC Technology for Mobile Communication Systems," presented at the 1998 IEEE MTT-S International Microwave Symposium (IMS 1998), Baltimore, 1998.
[16] X. Mi and S. Ueda, "Integrated Passives for High-Frequency Applications," in *Advanced Microwave Circuits and Systems*, V. Zhurbenko, Ed., ed: IntechOpen, 2010.
[17] T. Takai, H. Iwamoto, Y. Takamine, H. Yamazaki, T. Fuyutsume, H. Kyoya, T. Nakao, H. Kando, M. Hiramoto, T. Toi, M. Koshino, and N. Nakajima, "Incredible High Performance SAW Resonator on Novel Multi-Layerd Substrate," presented at the 2016 IEEE International Ultrasonics Symposium (IUS 2016), Tours, France, 2016.
[18] S. Inoue and M. Solal, "Spurious Free SAW Resonators on Layered Substrate with Ultra-High Q, High Coupling and Small TCF," presented at the 2018 IEEE International Ultrasonics Symposium (IUS 2018).
[19] O. Ikata, T. Nishihara, Y. Satoh, H. Fukushima, and N. Hirasawa, "A Design of Antenna Duplexer using Ladder Type SAW Filters," presented at the 1998 IEEE Ultrasonics Symposium (IUS 1998), 1998.
[20] M. Akiyama, T. Kamohara, K. Kano, A. Teshigahara, Y. Takeuchi, and N. Kawahara, "Enhancement of Piezoelectric Response in Scandium Aluminum Nitride Alloy Thin Films Prepared by Dual Reactive Cosputtering," *Adv. Mater.,* vol. 21, pp. 593-596, December 2008.
[21] T. Yanagitani, K. Arakawa, K. Kano, A. Teshigahara, and M. Akiyama, "Giant Shear Mode Electromechanical Coupling Coefficient k15 in c-axis Tilted ScAlN Films," presented at the 2010 IEEE International Ultrasonics Symposium (IUS 2010), San Diego, CA, USA, 2010.
[22] T. Yokoyama, Y. Iwazaki, Y. Onda, T. Nishihara, and M. Ueda, "Highly Piezoelectric Co-Doped AlN Thin Films for Bulk Acoustic Wave Resonators," presented at the 2013 IEEE International Ultrasonics Symposium (IUS 2013), Prague, Czech Republic, 2013.
[23] S. Manna, K. R. Talley, P. Gorai, J. Mangum, A. Zakutayev, G. L. Brennecka, V. Stevanović, and C. V. Ciobanu, "Enhanced Piezoelectric Response of AlN via CrN Alloying," *Phys. Rev. Applied,* vol. 9, 2018.
[24] G. Piazza, P. J. Stephanou, and A. P. Pisano, "Piezoelectric Aluminum Nitride Vibrating Contour-Mode MEMS Resonators," *IEEE/ASME Journal of Microelectromechanical Systems,* vol. 15, 2006.
[25] A. Konno, M. Sumisaka, A. Teshigahara, K. Kano, K.-y. Hashimo, H. Hirano, M. Esashi, M. Kadota, and S. Tanaka, "ScAlN Lamb Wave Resonator in GHz Range Released by XeF2 Etching," presented at the 2013 IEEE International Ultrasonics Symposium (IUS 2013), 2013.
[26] L. Colombo, A. Kochhar, C. Xu, G. Piazza, S. Mishin, and Y. Oshmyansky, "Investigation of 20% Scandium-doped Aluminum Nitride Films for MEMS Laterally Vibrating Resonators," presented at the 2017 IEEE International Ultrasonics Symposium (IUS 2017), 2017.
[27] C. Zuo, C. H. Yun, P. J. Stephanou, S.-J. Park, C.-S. T. Lo, R. Mikulka, J.-H. J. Lan, M. F. Velez, R. V. Shenoy, J. Kim, and M. M. Nowak, "Cross-sectional Dilation Mode Resonator with Very High Electromechanical Coupling up to 10% using AlN," presented at the 2012 IEEE International Frequency Control Symposium (IFCS 2012).
[28] Y. Hui, Z. Qian, and M. Rinaldi, "A 2.8 GHz Combined Mode of Vibration Aluminum Nitride MEMS Resonator with High Figure of Merit Exceeding 45," presented at the 2013 Joint European Frequency and Time Forum & International Frequency Control Symposium (EFTF/IFCS 2013), Prague, Czech Republic, 2013.
[29] C. Cassella and G. Piazza, "AlN Two-Dimensional-Mode Resonators for Ultra-High Frequency Applications," *IEEE Electron Device Letters,* vol. 36, pp. 1192-1194, November 2015.
[30] J. Segovia-Fernandez and C. Cassella, "Active and Inactive Frames Improve Figure of Merit of Two Dimensional Mode Resonators," presented at the 2018 IEEE International Ultrasonics Symposium (IUS 2018), Kobe, Japan, 2018.
[31] N. Wang, Y. Zhu, G. L. Chua, B. Chen, M. Srinivas, N. Singh, and Y. Gu, "Spurious Mode Free 3.5GHz AlN Plate Mode Resonator with High FoM," presented at the 2018 IEEE International Ultrasonics Symposium (IUS 2018), Kobe, Japan, 2018.
[32] Y. Osugi, T. Yoshino, K. Suzuki, and T. Hirai, "Single Crystal FBAR with LiNbO3 and LiTaO3 Piezoelectric Substance Layers," presented at the 2007 IEEE/MTT-S International Microwave Symposium (IMS 2007), Honolulu, HI, USA, 2007.
[33] M. Kadota, T. Ogami, K. Yamamoto, Y. Negoro, and H. Tochishita, "High Frequency Lamb Wave Device Composed of LiNbO3 Thin Film," presented at the 2008 IEEE Ultrasonics Symposium (IUS 2008).
[34] S. Gong, L. Shi, and G. Piazza, "High Electromechanical Coupling MEMS Resonators at 530 MHz using Ion Sliced X-cut LiNbO3 Thin Film," presented at the 2012 IEEE/MTT-S International Microwave Symposium (IMS 2012), Montreal, QC, Canada, 2012.
[35] M. Kadota, T. Ogami, K. Yamamoto, Y. Negoro, and H. Tochishita, "4.5 GHz Lamb wave device composed of LiNbO3 thin film," presented at the 2009 IEEE MTT-S International Microwave Symposium (IMS 2009), Boston, MA, USA, 2009.
[36] Y. Yang, A. Gao, R. Lu, and S. Gong, "5 GHz Lithium Niobate MEMS Resonators with High FoM of 153," presented at the 2017 IEEE 30th International Conference on Micro Electro Mechanical Systems (MEMS 2017), Las Vegas, NV, USA, 2017.
[37] Y. Jang, J.-D. Ha, S.-J. Lee, J. Lim, S.-M. Han, and D. Ahn, "Compact Size and Wideband Triplexer using SAW Resonators and LC Components," presented at the 2018 IEEE/MTT-S International Microwave Symposium (IMS 2018), Philadelphia, PA, USA, 2018.
[38] M. Wagner, T. Gossmannz, J. Tomasikz, R. Weigel, A. Hagelauer, and S. Leuschner, "A Hybrid Acoustic-Wave Resonator and Lumped-Element Ladder Filter," presented at the 2018 IEEE International Ultrasonics Symposium (IUS 2018), Kobe, Japan, 2018.
[39] J. D. Larson III, P. D. Bradley, S. Wartenberg, and R. C. Ruby, "Modified Butterworth-Van Dyke Circuit for FBAR Resonators and Automated Measurement System," presented at the 2000 IEEE International Ultrasonics Symposium (IUS 2000), 2000.